OPEN ACCESS

Laboratory science

Deep segmentation of OCTA for evaluation and association of changes of retinal microvasculature with Alzheimer's disease and mild cognitive impairment

Jianyang Xie ,[1] Quanyong Yi ,[2] Yufei Wu,[3] Yalin Zheng ,[4] Yonghuai Liu,[5] Antonella Macerollo,[6] Huazhu Fu ,[7] Yanwu Xu,[8] Jiong Zhang,[1] Ardhendu Behera,[5] Chenlei Fan,[9] Alejandro F Frangi,[10] Jiang Liu,[11] Qinkang Lu,[12] Hong Qi ,[13] Yitian Zhao[1]

► Additional supplemental material is published online only. To view, please visit the journal online (http://dx.doi.org/10.1136/bjo-2022-321399).

For numbered affiliations see end of article.

Correspondence to
Dr Yitian Zhao, Ningbo Institute of Materials Technology and Engineering Chinese Academy of Sciences, Ningbo, Zhejiang, 315201 P.R, China; yitian.zhao@nimte.ac.cn, Dr Hong Qi; doctorqihong@163.com and Dr Qinkang Lu; luqinkang@163.com

JX, QY and YW contributed equally.

Received 15 April 2022
Accepted 17 December 2022
Published Online First
3 January 2023

To cite: Xie J, Yi Q, Wu Y, *et al*. *Br J Ophthalmol* 2024;**108**:432–439.

ABSTRACT

Background Optical coherence tomography angiography (OCTA) enables fast and non-invasive high-resolution imaging of retinal microvasculature and is suggested as a potential tool in the early detection of retinal microvascular changes in Alzheimer's Disease (AD). We developed a standardised OCTA analysis framework and compared their extracted parameters among controls and AD/mild cognitive impairment (MCI) in a cross-section study.

Methods We defined and extracted geometrical parameters of retinal microvasculature at different retinal layers and in the foveal avascular zone (FAZ) from segmented OCTA images obtained using well-validated state-of-the-art deep learning models. We studied these parameters in 158 subjects (62 healthy control, 55 AD and 41 MCI) using logistic regression to determine their potential in predicting the status of our subjects.

Results In the AD group, there was a significant decrease in vessel area and length densities in the inner vascular complexes (IVC) compared with controls. The number of vascular bifurcations in AD is also significantly lower than that of healthy people. The MCI group demonstrated a decrease in vascular area, length densities, vascular fractal dimension and the number of bifurcations in both the superficial vascular complexes (SVC) and the IVC compared with controls. A larger vascular tortuosity in the IVC, and a larger roundness of FAZ in the SVC, can also be observed in MCI compared with controls.

Conclusion Our study demonstrates the applicability of OCTA for the diagnosis of AD and MCI, and provides a standard tool for future clinical service and research. Biomarkers from retinal OCTA images can provide useful information for clinical decision-making and diagnosis of AD and MCI.

WHAT IS ALREADY KNOWN ON THIS TOPIC

⇒ Retinal microvascular changes in optical coherence tomography angiography (OCTA) are believed as potential biomarkers for Alzheimer's disease (AD) and mild cognitive impairment (MCI) diagnosis, but the variations in equipment being used, statuses of patients and analysis methodology caused inconsistent results among published papers.

WHAT THIS STUDY ADDS

⇒ Developed a new automated standardised framework, driven by the recent advancements in deep learning, which can automatethe extraction of 12 retinal parameters from OCTA images, and further investigated their potential as retinal biomarkers for AD and MCI.

HOW THIS STUDY MIGHT AFFECT RESEARCH, PRACTICE OR POLICY

⇒ We provides a standard tool for OCTA analysis, which can be used in future clinical service and research in AD and other applications.

BACKGROUND

The retina and the brain share similar physiological characteristics, embryology origin, precise neuron cell layers and microvasculature. With the increasing prevalence of Alzheimer's disease (AD) worldwide, recent reports suggest the retina as a potential route to evaluate and monitor the disease progression. Accumulating retinal imaging reports using different imaging tools suggested the neuronal integrity and microvasculature of the retina reflect that of the brain.[1 2] Compared with the current diagnostic gold standards such as positron emission tomography and spinal-fluid examination, retinal imaging is faster, non-invasive, affordable and accommodating to patients.[3] Reports suggested that the retina can be used as a window to study (AD) and other common neurodegenerative diseases.[4–6]

With the vast improvement in resolution of images and the accessibility of ophthalmological imaging tools, application of new, high resolution imaging tools such as the optical coherence tomography angiography (OCTA) have enabled the in vivo visualisation of the retinal microvasculature.[7] Of note, the use of OCTA in the early detection of retinal microvascular changes in AD is an area receiving growing scientific attention as witnessed by the sheer increase in the number of reports in the past few years.[8–16] However, there are inconsistencies across these reports, which may due

to the variations of equipment used, statuses of patients and most importantly methodology of analysis. The development of computational tools, such as deep learning algorithms has enhanced the potential of data-rich retinal imaging as a promising tool and a potential biomarker for AD.

In this study, we proposed a new standardised framework, driven by advances in deep learning for automated analysis of OCTA images. We extracted 12 different parameters characterising both retinal microvasculature and foveal avascular zone (FAZ). We also assessed the correlation between retinal microvascular changes and clinical features in AD and mild cognitive impairment (MCI).

METHOD

AD and MCI participants

Enrolled patients meet the National Institute on Aging and Alzheimer's criteria[17] for probable AD and the Petersen criteria[18] for MCI. Experienced neurologist made the diagnosis for the AD/MCI subjects, specifically, enrolled AD patients had Mini Mental State Examination (MMSE) scores within 13–20 while MCI patients had MMSE scores within 21–24. The criteria for exclusion of participants were those with neurodegenerative diseases (such as Parkinson's disease), psychiatric disease, toxic or metabolic disease, infectious disease, ophthalmic disease (examined by an experienced ophthalmic according to the fundus and OCTA images of the patients without knowing their health statuses) which could not permit the imaging of the macula (severe glaucoma and cataract), diabetic retinopathy, corneal opacities, elevated intraocular pressure, optic neuropathy or high myopia (>6.0 D).

Control group

Healthy participants had similar educational background, age and sex to the AD and MCI participants. Participants were excluded if they were hypotensive, or uncontrolled hypertensive; experienced neurological disorders; or reported current or previous substance abuse. All received MMSE examination and had scores of over 24.

OCT angiography image acquisition

Macula microvascular imaging was acquired with using OCTA device (Avanti RTVue XR, Optovue, Fremont, California, USA, software V.2017.1.0.151). The imaging camera is capable of scanning at 70 000 A-scans/s with an axial resolution of 5 µm and a light source with wavelength 840±10 µm. The macula of each participant was assessed by using B-scans covering an area of $3\times3\,mm^2$ and $6\times6\,mm^2$ horizontally and vertically. An inbuilt software in the OCTA camera was used to project the macula microvasculature into the superficial vascular complex (SVC), deep vascular complex (DVC) and inner retinal vascular complex (IVC), as shown in figure 1B. The OCTA tool (software V.2017.1.0.151) was incorporated with a three-dimensional Projection Artefact Removal (3D PAR) to reduce projection artefacts in the deeper capillary plexus while preserving the authentic layout. The SVC and DVC were set in the inner two-thirds and the outer one-third interface of the ganglion cell layer (GCL) and inner plexiform layer. IVC consists of the SVC and DVC and was defined as 5 µm above the inner limiting membrane to 25 µm below the border of the inner nuclear layer, as shown in figure 1A.

Deep learning-based extraction of microvasculature and FAZ

We proposed a standard tool for the automated analysis of OCTA images: Two deep learning-based approaches are employed for the accurate segmentation of microvasculature and FAZ from OCTA images, respectively. The segmentations will be used to extract the parameters of interest of microvasculature and FAZ thereafter.

Microvasculature segmentation

We used a state-of-the-art method, OCTA-Net[19] for microvasculature segmentation in OCTA images. This model consists of a split-based coarse segmentation and a split-based refining segmentation module, with the goal of producing a preliminary confidence map, and optimising the contour of the retinal microvasculature, respectively. The OCTA-Net was trained on a public OCTA dataset named ROSE-1, and its efficiency has been validated, with its AUC >0.940.[19] The dataset contains 117 OCTA en face angiograms (example shown in figure 1C) acquired using the RTVue XR Avanti SD-OCT system. Clinicians manually annotated all microvasculatures as the ground truth at pixel and centreline level. In this study, 60 images were used for training the OCTA-Net and the rest for testing. Figure 1D illustrates an example of the microvascular segmentation. We have provided more details about the OCTA-Net in online supplemental appendix 1.

FAZ segmentation

A gate-based feature integration deep network (FAZ-Net) is employed for the FAZ segmentation.[20] This method was inspired by an ensemble model.[21] Three encoders are designed to obtain features intelligently integrated by voting to enhance the robustness and representation ability of features. We invited a senior ophthalmologist to manually trace the FAZ boundary in each OCTA image of the ROSE-1 dataset. We used 60 images for training and the rest for testing the FAZ-Net. The segmentation performance has shown its robustness and effectiveness, with Dice>0.95. Figure 1K illustrates an example of the FAZ segmentation. The brief descriptions of the FAZ-Net are provided in online supplemental appendix 2.

Definitions of quantitative parameters

We defined and investigated 12 parameters that represent the distribution, topology, orientation and shape of both microvasculature and the FAZ, as illustrated in figure 1.

Vascular-related parameters

Vascular area density: The total length in millimetres of perfused retinal microvasculature per unit area in square millimetres in the annular region of the analysed area.[16]

Vascular length density: The ratio between the total number of pixels of microvascular centreline (shown in figure 1E) and the area of the analysed region.

Vascular fractal dimension (VFD): A well-known measure of the geometric complexity of vasculature, as shown in figure 1G.

Vascular tortuosity: A metric to measure the tortuous level of the vasculature as shown in figure 1I, computed by applying the method proposed by Zhao *et al*.[22]

Vascular bifurcation number: The total number of bifurcations, which are determined by locating the intersection points of the vessel map at centreline level, as shown in figure 1F (pixels with more than two neighbours).

Vascular orientation distribution: Calculates the direction of each vascular pixel to indicate the trend of the blood flow, as shown in figure 1H. More details about vascular orientation distribution are in online supplemental appendix 3.

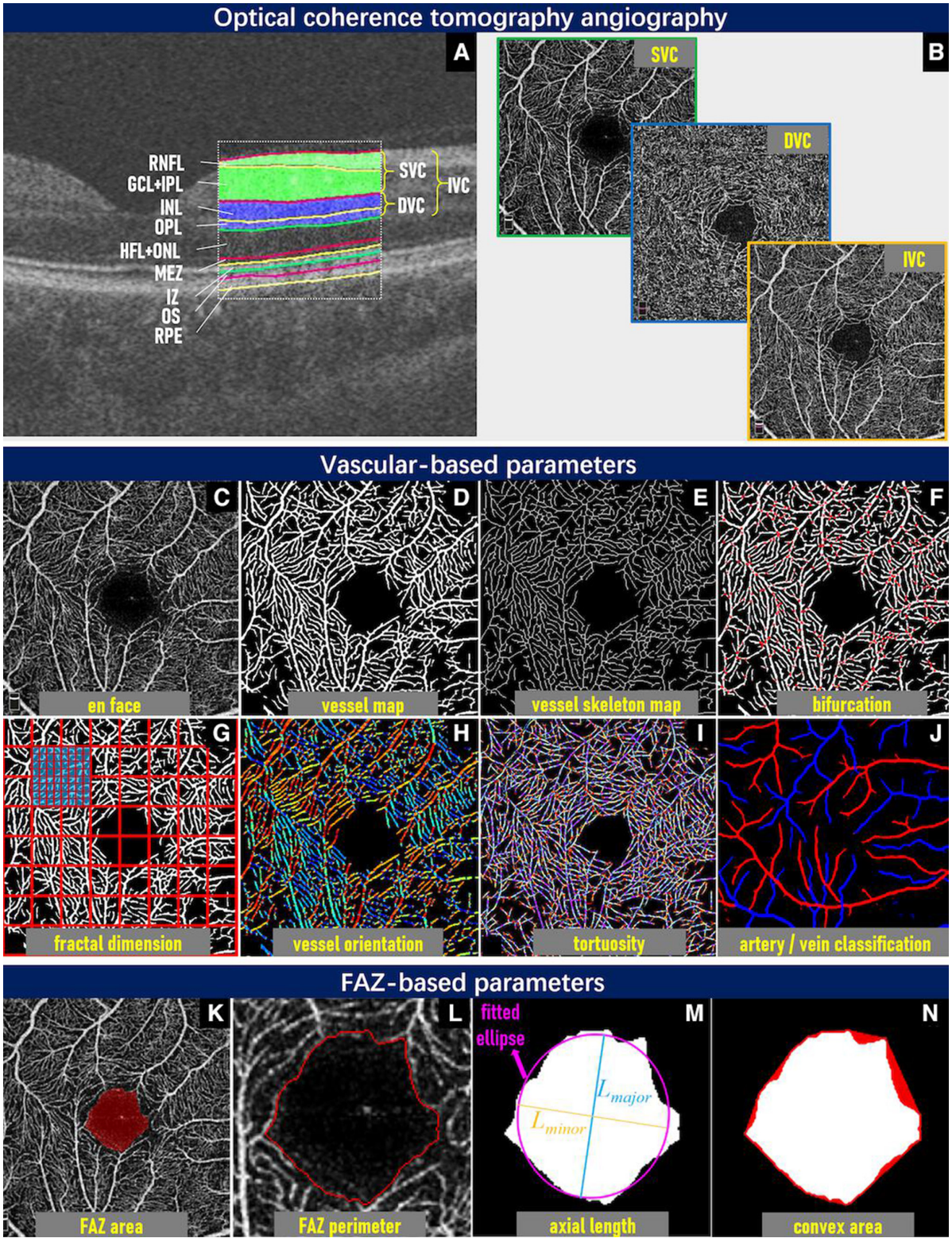

Figure 1 Vascular and foveal avascular zone (FAZ)-related parameters used in the quantitative measurements. (A) Illustrates a B-scan of a sample OCT volume with retinal layers illustrated. (B) Are en face angiograms of superficial vascular complexes (SVC), deep vascular complexes (DVC) and inner vascular complexes (IVC), respectively. (C) Shows a 3×3 mm^2 en face SVC angiogram. (D, E) Show the automated segmented vessel map and vessel skeleton map of (C), respectively. By calculating the ratio of vasculatures in (D) and (E), vascular area density (VAD) and vascular length density (VLD) can be derived, respectively. The red dots in (F) indicate the vascular bifurcations (VB). (G–J) Illustrate vascular fractal dimension (VFD), vascular orientation distribution (VOD), vascular tortuosity (VT) and arterioles/venules (AV) classification, respectively. (Note: the AV classification is only applied to the 6×6 mm^2 en face angiogram in this work.) (K) Is the detected FAZ area (FA), and (l) shows its perimeter (FP). The circularity of the FAZ (FC) is calculated as: $FC=4\pi * FA/FP^2$. (M) Shows the major and minor axes of the fitted ellipse of the FAZ. The axis ratio of the FAZ (FAR) is defined as the ratio between major axial length L_{major} and minor axial length L_{minor}, while the roundness of the FAZ (FR) is calculated via $FR=4\pi * FA/ L^2$. (N) Shows the convex area of the FAZ, and the solidity of the FAZ (FS) is defined as the ratio between the FA and the convex area.

Arterioles and venules caliber ratio (AVR): The ratio of mean calibres between arterioles and venules. Note that the AVR is calculated in 6×6 mm^2 OCTA images only, by using the method proposed by Xie *et al*[23] to distinguish automatically between arteries and veins, as shown in figure 1J.

FAZ-related parameters

FAZ area: The total number of pixels in the FAZ region.

FAZ axis ratio: The ratio between the major and minor axes of the fitted ellipse from the FAZ boundary, as shown in figure 1M. A higher FAR indicates an elongated FAZ with greater eccentricities.

FAZ circularity: The degree of roundness of the FAZ.[24] The larger the FC value, the more circular the shape. A value of 1.0 denotes a perfect circle.

FAZ roundness: Similar to FC, but is less sensitive to irregular borders along the perimeter (shown in figure 1L) of FAZ.

FAZ solidity: Describes the extent to which the FAZ is convex or concave as shown in figure 1N, and is defined as the ratio between the FA and the convex area covering the FAZ. The further the solidity deviates from 1, the greater the extent of concavity in the structure.

Statistical analyses

In this study, only one eye per individual was used for the analysis, to avoid between-eye correlation. The eye with higher signal strength intensity (SSI) and visual acuity (VA) was selected when images of both eyes are available. The demographic variables of enrolled participants and the extracted OCTA parameters were compared across the three groups. If the samples across each group met the hypothesis of homogeneity of variance, one-way analysis of variance (ANOVA) was performed for continuous variables; otherwise, a non-parametric test was applied for continuous variables and a Chi-square test for categorical variables. Furthermore, considering the impact of confounding factors (such as image quality, other eye disease), OCTA parameters were modelled using the continuous and multivariate logistic regression (MLR) method. The Bonferroni correction was performed in our result. In practice, the p Value for SVC and IVC was corrected by 24, and the p value for DVC was corrected by 12. All statistical analyses were performed using the SPSS software (V.22.0; SPSS), and a $p<0.05$ (two sided) was considered statistically significant.

RESULTS

Descriptive Statistics

A total of 55 AD, 62 healthy control (HC) and 41 MCI participants were enrolled. Ten AD and three HC participants were excluded, because of low signal quality during imaging and/or presence of imaging artefacts. This analysis thus consisted of 45 eyes of AD participants, 41 eyes of MCI and 59 eyes of HC.

As shown in table 1, there are no significant difference ($p\geq0.05$) in terms of age and diabetic status among the three groups in the ANOVA analysis. In the univariate logistic regression analysis, the MCI patients are older than the controls, but there is no significant age difference between AD and healthy controls. There is a significant difference in gender ratios ($p=0.029$) between the three groups. The univariate logistic regression analyses showed that both the AD and MCI groups have significantly reduced MMSE scores ($p<0.001$) compared with HC. Due to the incomplete demographic information of the MCI group, the education level, hypertension and SSI parameters were only compared between AD and HC groups. A significant difference ($p<0.05$) is found in education level, while there is no significant difference in hypertension and SSI ($p>0.05$) between the AD and HC groups.

The OCTA parameters were compared within the three groups: the results are shown in table 2. In the DVC, VAD, VLD and VFD are significantly reduced ($p<0.05$) in AD and MCI when compared with HC, and the FR shows a significant difference ($p=0.014$) between the three groups. In the SVC, there are significant differences in VAD, VLD, VFD, VB and FR ($p<0.05$) among the three groups. In the IVC, there are no significant difference in FAZ- related parameters between AD, MCI and controls, while the VAD, VLD, VFD and VB showed significant decreases ($p<0.05$) in AD and MCI compared with HC participants. Of note, VT in IVC shows significant difference among the three groups ($p=0.007$).

In the 6×6 mm^2 fovea-centred scans, no significant differences among the three groups are found in AVR.

Logistic regression analysis

After adjusting the demographic data, the results of the MLR analysis are shown in table 3. In the DVC, the changes in OCTA parameters are not significantly associated ($p\geq0.05$) with the presence of MCI or AD. In the SVC, the decrease of VAD, VLD, VFD and VB, and the change in FR shows a significant

Table 1 Results of univariate logistic regression for demographic data

Variable	HC (N=59) Mean (SD)	MCI (N=41) Mean (SD)	OR	95% CI	P_1	AD (N=45) Mean (SD)	OR	95% CI	P_2	P value
Age, year	58.73 (6.91)	61.73 (7.84)	1.064	1.004 to 1.128	0.038	60.60 (6.265)	1.040	0.983 to 1.100	0.175	0.098*
No of females (%)	35 (46.7)	14 (34.1)	0.356	0.155 to 0.814	0.014	26 (57.8)	0.938	0.427 to 2.062	0.874	0.029†
MMSE	26.52 (3.14)	21.09 (3.91)	0.685	0.586 to 0.799	<0.001	13.89 (5.40)	0.497	0.401 to 0.617	<0.001	<0.001‡
Diabetes (%)	2 (3.3)	2 (4.9)	0.684	0.092 to 5.065	0.710	2 (4.4)	0.737	0.100 to 5.445	0.765	0.928†
Education level	1.441 (0.82)	–	–	–	–	1.977 (1.09)	1.831	1.179 to 2.844	0.007	0.004‡
Hypertension	13 (21.3)	–	–	–	–	3 (7.3)	4.252	1.139 to 15.865	0.031	0.057§
SSI	8.26 (0.83)	–	–	–	–	8.07 (0.85)	0.568	0.357 to 0.902	0.017	0.368§

Continuous variables were described by mean (SD), and frequencies (percentages) were used to describe categorical variables. P_1 and P_2 were calculated by univariate logistic regression analysis between MCI and HC, AD and HC respectively. P was a comparison result among the three groups of AD, MCI and HC.
*P value was obtained by ANOVA.
†The p value was obtained via χ^2 test.
‡The p value was obtained non-parametric tests.
§P value was obtained by Student's t-test.
AD, Alzheimer's diseases; ANOVA, analysis of variance; HC, healthy controls; MCI, mild cognitive impairment; MMSE, Mini Mental State Examination; SSI, signal strength intensity.

Table 2 Comparisons of OCTA parameters between healthy control, MCI and AD participants

		DVC				SVC				IVC		
Variable	AD	MCI	Control	P value	AD	MCI	Control	P value	AD	MCI	Control	P value
VAD	23.82 (4.98)	22.06 (4.67)	25.06 (5.05)	**0.027**	15.51 (2.25)	15.35 (2.59)	16.65 (2.32)	**0.014**	15.72 (3.24)	16.03 (3.36)	18.06 (2.92)	**<0.001**
VLD	9.32 (1.83)	8.70 (1.71)	9.81 (1.80)	**0.027**	5.74 (0.89)	5.61 (1.00)	6.17 (0.92)	**0.009**	5.92 (1.30)	5.98 (1.31)	6.85 (1.14)	**<0.001**
VFD	1.58 (0.05)	1.57 (0.06)	1.59 (0.04)	**0.022**	1.49 (0.04)	1.48 (0.04)	1.50 (0.03)	**0.017**	1.49 (0.05)	1.49 (0.05)	1.52 (0.04)	**0.001***
VT	1.56 (0.12)	1.54 (0.15)	1.54 (0.13)	0.577	1.80 (0.22)	1.86 (0.30)	1.73 (0.26)	0.059	1.86 (0.33)	1.87 (0.27)	1.70 (0.28)	**0.007**
VB	243(68)	220(64)	249(64)	0.433	141(36)	133(38)	157(35)	**0.003**	134(41)	132(36)	161(36)	**<0.001**
VOD	0.80 (0.03)	0.80 (0.04)	0.79 (0.04)	0.486	0.85 (0.06)	0.85 (0.05)	0.85 (0.06)	0.942	0.84 (0.06)	0.84 (0.06)	0.83 (0.07)	0.952
AVR	—	—	—	—	—	—	—	—	0.99 (0.06)	0.10 (0.07)	0.99 (0.08)	0.761
FA	0.37 (0.12)	0.33 (0.11)	0.34 (0.12)	0.354	0.75 (0.21)	0.65 (0.26)	0.69 (0.20)	0.129	0.39 (0.14)	0.35 (0.12)	0.37 (0.12)	0.462
FAR	1.07 (0.28)	1.20 (0.18)	1.12 (0.19)	0.144	1.13 (0.39)	1.17 (0.55)	1.22 (0.22)	0.431	1.20 (0.39)	1.15 (0.25)	1.14 (0.25)	0.555
FR	40.03 (9.29)	34.79 (4.82)	37.57 (7.03)	**0.014***	39.58 (10.75)	40.30 (13.27)	34.42 (7.00)	**0.010***	36.26 (8.41)	37.26 (8.73)	37.27 (7.50)	0.501
FC	0.95 (0.12)	0.99 (0.11)	0.98 (0.11)	0.205	0.70 (0.11)	0.71 (0.17)	0.74 (0.111)	0.081*	0.93 (0.12)	0.94 (0.14)	0.93 (0.13)	0.936
FS	0.93 (0.04)	0.94 (0.04)	0.94 (0.03)	0.602	0.85 (0.03)	0.86 (0.06)	0.86 (0.05)	0:357*	0.92 (0.04)	0.92 (0.06)	0.92 (0.05)	0.100

Note: the p value was obtained by ANOVA.
*The p value was obtained by non-parametric tests. AVR was analysed in the 6×6 mm^2 fovea centred scans.
AD, Alzheimer's disease; ANOVA, analysis of variance; AVR, arterioles/venules diameter ratio; DVC, deep vascular complexes; FA, FAZ area; FAR, axis ratio of the FAZ; FC, Circularity of the FAZ; FP, FAZ perimeter; FR, roundness of the FAZ; FS, solidity of the FAZ; IVC, inner vascular complexes; MCI, mild cognitive impairment; SVC, superficial vascular complexes; VAD, vascular area density; VB, vascular bifurcations; VFD, vascular fractal dimension; VLD, vascular length density; VOD, vascular orientation distribution; VT, vascular tortuosity.

correlation ($p<0.05$) with the presence of MCI. In the IVC, decreased VAD, VLD and VB significantly correlate with the presence of AD or MCI ($p<0.05$). Furthermore, increased VT and decreased VFD only show significant correlation ($p<0.05$) with the presence of MCI. There was no association between changes in FAZ-related-parameters and AD or MCI ($p\geq0.05$).

DISCUSSION

Microvascular alterations in AD individuals versus in healthy controls

In this study, OCTA techniques are used to analyse the retinal vascular morphology and vascular density in AD, MCI and controls. The AD participants show decreased microvascular density and damage vascular morphology in terms of VAD, VLD and VB in the IVC when compared with controls, whereas there is no significant structural difference in the DVC and SVC. Although our findings are not in line with most OCTA studies shown in table 4, our study suggests that microvascular impairment occurs in the pathogenesis of AD.

Our results in table 3 show that AD participants have as impaired microvascular morphology and densities in the SVC and DVC, but no significant difference is observed. This finding is discordant with the conclusions of most previous studies,[9–11 13 15 16] where AD participants showed a decrease in microvascular density compared with controls. However, there are also some studies that support our result.[12 14] Possible explanations for this phenomenon are suggested below.

On one hand, the decreasing density of the vasculature may be due to β- Amyloid (A-β) deposits, which have been reported by Brown *et al*.[25] In their work, they argued that A-β deposition around vascular walls disrupts the basement membrane of small vessels, causing endothelial damage and thus reducing angiogenesis. First, the decreasing density of vasculature observed in our study did not reach a significant level. This may be related to several confounders. First, the absence of motion artefacts and high software-derived image quality scores (>6/10) were necessary to obtain good or excellent repeatability for performing the vascular measurement.[26] In our study, images with scan qualities below 7, or with artefacts were excluded, and the SSIs are thus highly similar between the AD group and the controls (8.26 vs 8.07). Second, differences in the instruments and embedded software used may cause inconsistencies between different studies. Spaide and Curcio[27] analysed three different instruments (Carl Zeiss, Optovue and Topcon) in terms of the segmentation slab, designed to isolate the superficial vascular plexus and the deep vascular plexus, and pointed out that three different instruments produced differing segmentation results. Meanwhile, when directly comparing the images captured by OCTA with the vascular patterns in an autopsied eye, they concluded that none of the instruments produced segmented regions that correctly followed the relevant anatomic layers.

The IVC in our study was the layered combination of DVC and SVC, and the vascular parameters of AD participants showed significant decrease when compared with controls. This may be attributed to the accumulation of the different changes in the SVC and DVC, as the changes in value in the SVC and DVC when considered separately did reach a significant level in our study. Therefore, vasculature parameter measurement in the IVC may be more promising in investigating the AD. However, there is only one study[13] working on the IVC slab, and in this work the SSI was not adjusted.

Microvascular alterations in MCI individuals versus in healthy controls

Our results imply that MCI participants exhibit significant vessel loss (ie, decreases in VAD, VLD, VFD and VB values) in the SVC when compared with control participants, but no significant vasculature decrease is observed in the DVC, which supports some of the previous findings in MCI participants.[15 16] This finding may indicate that the SVC, which is responsible for the metabolic demands of the parafoveal GCL,[28 29] is the target of pathology in MCI. Therefore, we conjecture that the change in the DVC may occur after the alteration in the SVC. However, there are studies[13 14] that reach the opposite conclusion: capillary alterations occur only in the DVC.

Conflicting results within different studies may be due to other reasons. Except for the effects of varied image quality, artefacts and instruments, the inconsistent results between previous studies may be also due to excessively vague selection standards for the MCI participants. MCI is a period during which, as cognitive decline gradually progresses from normal to dementia, individuals may suffer from a

Table 3 Results of multivariate logistic regression analysis

	DVC			SVC			IVC		
Variable	OR	95% CI	P value	OR	95% CI	P value	OR	95% CI	P value
VAD									
MCI	0.906	0.817 to 1.004	0.059	0.812	0.667 to 0.989	**0.038**	0.823	0.707 to 0.959	**0.013**
AD	0.957	0.800 to 1.146	0.635	0.825	0.629 to 1.082	0.164	0.699	0.661 to 0.965	**0.020**
VLD									
MCI	0.752	0.565 to 1.002	0.052	0.564	0.341 to 0.934	**0.026**	0.586	0.396 to 0.868	**0.008**
AD	0.934	0.525 to 1.663	0.816	0.680	0.337 to 1.372	0.282	0.575	0.354 to 0.934	**0.025**
VFD									
MCI	0.000	0.000 to 5.314	0.097	0.006	0.000 to 0.384	**0.036**	0.003	0.000 to 0.069	**0.014**
AD	0.030	0.003 to 1.173e^{5}	0.651	0.001	0.000 to 4.212e^{4}	0.421	0.010	0.000 to 1.929	0.063
VT									
MCI	0.477	0.020 to 11.407	0.648	8.393	0.917 to 31.709	0.062	7.542	1.251 to 45.461	**0.027**
AD	3.065	0.609 to 15.424	0.174	2.291	0.231 to 22.751	0.479	3.449	0.532 to 22.382	0.194
VB									
MCI	0.995	0.988 to 1.003	0.201	0.981	0.968 to 0.995	**0.007**	0.980	0.967 to 0.993	**0.002**
AD	0.993	0.975 to 1.011	0.430	0.987	0.969 to 1.005	0.162	0.984	0.970 to 0.998	**0.023**
VOD									
MCI	1.382e^{3}	0.006 to 3.370e^{8}	0.253	11.056	0.005 to 2.284e^{4}	0.537	2.641	0.002 to 2.940e^{3}	0.786
AD	0.046	0.000 to 4.995	0.198	0.609	0.000 to 1.295e^{3}	0.899	6.747	0.004 to 1.151e^{4}	0.615
AVR									
MCI	—	—	—	—	—	—	7.409	0.009 to 5.851e^{3}	0.468
AD	—	—	—	—	—	—	1.226	0.003 to 0.511e^{3}	0.947
FA									
MCI	0.739	0.275 to 1.986	0.548	0.790	0.470 to 1.329	0.374	0.712	0.281 to 1.80^{3}	0.474
AD	10.500	0.000 to 5.566e^{5}	0.672	1.499	0.839 to 2.679	0.172	1.811	0.726 to 4.518	0.203
FAR									
MCI	3.257	0.428 to 24.789	0.254	0.392	0.227 to 2.111	0.518	1.224	0.245 to 6.102	0.805
AD	1.042	0.835 to 1.300	0.716	0.443	0.108 to 1.825	0.260	1.265	0.280 to 5.713	0.760
FR									
MCI	0.942	0.875 to 1.013	0.107	1.069	1.107 to 1.123	**0.008**	0.992	0.941 to 1.046	0.771
AD	1.000	0.999 to 1.001	0.714	1.052	0.994 to 1.113	0.081	0.998	0.942 to 1.058	0.952
FC									
MCI	2.744	0.061 to 122.695	0.603	0.147	0.005 to 4.360	0.268	3.306	0.107 to 102.420	0.495
AD	0.424	0.049 to 3.696	0.437	0.084	0.001 to 6.011	0.255	4.193	0.104 to 169.616	0.448
FS									
MCI	0.191	0.004 to 2.095e^{4}	0.315	0.022	0.006 to 190.172	0.408	0.347	0.041 to 1.980e^{3}	0.811
AD	22.168	0.126 to 3.911e^{3}	0.240	0.007	0.001 to 446.681	0.380	50.296	0.001 to 1.722e^{6}	0.462

P value of AD was adjusted for age, education level, hypertension and signal strength of OCTA scans; p value of MCI was adjusted for age, gender and diabetes. AVR was analysed only for the 6×6 mm^2 OCTA images.
AVR, arterioles/venules diameter ratio; DVC, deep vascular complexes; FA, FAZ area; FAR, axis ratio of the FAZ; FC, circularity of the FAZ; FP, FAZ perimeter; FR, roundness of the FAZ; FS, solidity of the FAZ; IVC, inner vascular complexes; MCI, mild cognitive impairment; OCTA, optical coherence tomography angiography; SVC, superficial vascular complexes; VAD, vascular area density; VB, vascular bifurcations; VFD, vascular fractal dimension; VLD, vascular length density; VOD, vascular orientation distribution; VT, vascular tortuosity.

wide range of cognitive impairments, even if they can still carry out their activities of daily living with no help from others.[30] Therefore, the heterogeneity of vascular alterations in different stages of MCI may explain inconsistent findings between studies. In addition, MCI vasculature alteration in the IVC may be more predictive than in the other two slabs, as we observed significant decreases in VAD, VLD, VFD, VB and VT values in the IVC.

FAZ alterations between AD/MCI and control

In our study, there is no association between AD/ MCI and FAZ-related parameters in all three plexuses except for the FR in the SVC of MCI. Our finding contradicts the findings of some previous studies (table 4). This inconsistency may be multifaceted since the FAZ area has numerous limitations when considered a potential biomarker. For example, some studies[31] have shown that age, gender and eyeball axial length can affect the FAZ area. Therefore, it is necessary to adjust the age, gender and axial length parameters when analysing FAZ-related parameters between different groups. To this end, age and gender were adjusted in this study for the multivariate regression analysis, which may explain why our findings differ from those of others. In addition, the significant alteration of FR in the SVC may support the conclusion that the roundness of the FAZ may be a potential biomarker in MCI diagnosis, as this parameter is less related to the absolute size of the FAZ, and to the axial length of the eyeball.

Table 4 Optical coherence tomography angiography (OCTA) studies on individuals with Alzheimer's disease (AD) and mild cognitive impairment

Authors	Participants	OCTA device	Scan area mm^2	Parameters	SVC	DVC	IVC
O'Bryhim *et al*[8]	14 AD 16 control	RTVue XR Avanti	8×8	FA	Not analysed.	Not analysed.	FAZ ↑ in AD
Bulut *et al*[9]	26 AD 26 control	RTVue XR 100–2	6×6	VAD, FA	VAD ↓ in AD FA ↑ in AD	Not analysed.	Not analysed.
Yoon *et al*[10]	39 AD 37 MCI 133 control	Cirrus HD-5000	3×3 6×6	VAD, FA	VAD ↓ in AD	Not analysed.	Not analysed.
Lahme *et al*[11]	36 AD 38 control	RTVue XR Avanti	3×3	VAD	VAD ↓ in AD	No significant difference.	Not analysed.
Zabel *et al*[12]	27 AD 27 control	RTVue XR Avanti	6×6	VAD, FA	No significant difference.	VAD ↓ in AD FA ↑ in AD	Not analysed.
Hong *et al*[13]	12 AD 19 MCI 21 control	Cirrus HD-5000	3×3 6×6	VFD	VFD ↓ in AD	VFD ↓ in AD VFD ↓ in MCI	VFD ↓ in AD
Wu *et al*[14]	18 AD 21 MCI 21 control	RTVue XR Avanti	6×6	VAD, FA	No significant difference.	VAD ↓ in AD VAD ↓ in MCI FA ↑ in AD FA ↑ in MCI	Not analysed.
Zhang *et al*[15]	16 AD/MCI 16 control	RTVue XR Avanti	3×3	VAD, VLD	VAD ↓ in AD VAD ↓ in MCI	No significant difference.	Not analysed.
Chua *et al*[16]	24 AD 37 MCI 29 control	Cirrus HD-5000	3×3	VAD, VFD FA	VAD ↓ in AD VAD ↓ in MCI	VAD ↓ in AD	Not analysed.
Our work	45 AD 41 MCI 59 control	RTVue XR Avanti	3×3 6×6	As shown in section 2.5.	VAD ↓ in MCI VLD ↓ in MCI VFD ↓ in MCI VB ↓ in MCI FR ↑ in MCI	No significant difference.	VAD ↓ in MCI, AD VLD ↓ in MCI, AD VB ↓ in MCI, AD VFD ↓ in MCI VT ↑ in MCI

Note: ↑ and ↓ represent a significant increase and decrease compared with the control group. The parameters used have been detailed in section 2.5.
DVC, deep vascular complexes; FA, FAZ area; FAR, axis ratio of the FAZ; FC, Circularity of the FAZ; FP, FAZ perimeter; FR, roundness of the FAZ; FS, solidity of the FAZ; IVC, inner vascular complexes; SVC, superficial vascular complexes; VAD, vascular area density; VB, vascular bifurcations; VFD, vascular fractal dimension; VLD, vascular length density; VOD, vascular orientation distribution; VT, vascular tortuosity.

Limitations

This study has several limitations. First, despite employing the largest participant cohort of any related study, the number of participants is still relatively small. A cross-sectional study does not measure changes in retinal microvascular parameters over time or disease progression. Longitudinal studies in larger cohorts must determine whether these findings are a reliable method for identifying AD/MCI patients in the preclinical stage. Second, the data on eyeball axial length, usually used to identify myopia, were not acquired in this study: this may influence the area of OCTA captured, and thus introduce bias in estimating the vascular parameters, and subsequent analysis. However, all patients with high myopia were excluded from the study, we expect that the effects of axial length might be limited. Finally, some risk factors for MCI are lost and are not adjusted in MLR analysis, which might be optimised in future work.

Author affiliations
[1]Cixi Institute of Biomedical Engineering, Ningbo Institute of Materials Technology and Engineering, Chinese Academy of Sciences, Ningbo, Zhejiang, China
[2]Ningbo Eye Hospital, Ningbo, Zhejiang, China
[3]Department of Ophthalmology, The Affiliated People's Hospital of Ningbo University, Ningbo, Zhejiang, China
[4]Department of Eye and Vision Science, University of Liverpool, Liverpool, UK
[5]Department of Computer Science, Edge Hill University, Ormskirk, UK
[6]Institute of Systems, Molecular and Integrative Biology, University of Liverpool, Liverpool, UK
[7]Institute of High Performance Computing, Agency for Science, Technology and Research (A*STAR), Singapore
[8]Intelligent Healthcare Unit, Baidu Inc, Beijing, Haidian, China
[9]Department of Neurology, The Affiliated People's Hospital of Ningbo University, Ningbo, Zhejiang, China
[10]School of Computing, University of Leeds, Leeds, UK
[11]Department of Computer Science and Engineering, Southern University of Science and Technology, Shenzhen, Guangdong, China
[12]Department of Ophthalmology, Wenzhou Medical University, Wenzhou, Zhejiang, China
[13]Ophthalmology, Peking University Third Hospital, Haidian, Beijing, China

Contributors JX contributed to the experimental design, OCTA analysis, clinical analysis and manuscript writing. YW, YX, QY and Q-KL contributed to the revision and provided important intellectual content. YW and HQ contributed to the ophthalmic examination for participation and experimental design. YZ, YL, AM, AB and AFF contributed to the manuscript writing. HF and JL contributed to the experimental design and manuscript writing. JZ contributed to the OCTA analysis. CF contributed to the diagnosis of AD/MCI subjects. YZ contributed to the experimental design, OCTA analysis and manuscript writing. YZ is guarantor.

Funding This work was supported in part by the National Natural Science Foundation of China(62272444); Zhejiang Provincial Natural Science Foundation (LR22F020008); Youth Innovation Promotion Association CAS (2021298); Ningbo Major Science and Technology Task Project(2021Z054, 2021Z134); Medical Science and Technology Program of Zhejiang Province (2023KY1145)

Disclaimer The sponsor or funding organisation had no role in the design or conduct of this research.

Competing interests None declared.

Patient consent for publication Consent obtained directly from patient(s).

Ethics approval The clinical protocol of our study was approved by the ethics committee of the Cixi Institute of Biomedical Engineering, Chinese Academy of Sciences, and adhered to the principles of the Declaration of Helsinki. The study was conducted at the Affiliated People's Hospital of Ningbo University Hospital and Peking University Third Hospital. Participants enrolled in our study provided informed written consent.

Provenance and peer review Not commissioned; externally peer reviewed.

Data availability statement Data may be obtained from a third party and are not publicly available.

ORCID iDs
Jianyang Xie http://orcid.org/0000-0002-4565-5807
Quanyong Yi http://orcid.org/0000-0002-9369-3998
Yalin Zheng http://orcid.org/0000-0002-7873-0922
Huazhu Fu http://orcid.org/0000-0002-9702-5524
Hong Qi http://orcid.org/0000-0003-3066-8020

REFERENCES

1 Patton N, Aslam T, Macgillivray T, *et al*. Retinal vascular image analysis as a potential screening tool for cerebrovascular disease: a rationale based on homology between cerebral and retinal microvasculatures. *J Anat* 2005;206:319–48.
2 Ravi Teja KV, Tos Berendschot T, Steinbusch H, *et al*. Cerebral and retinal neurovascular changes: a biomarker for Alzheimer's disease. *J Gerontol Geriatr Res* 2017;6. doi:10.4172/2167-7182.1000447. [Epub ahead of print: 08 09 2017].
3 Grossman I, Lutz MW, Crenshaw DG, *et al*. Alzheimer's disease: diagnostics, prognostics and the road to prevention. *Epma J* 2010;1:293–303.
4 Skrobot OA, Black SE, Chen C, *et al*. Progress toward standardized diagnosis of vascular cognitive impairment: guidelines from the vascular impairment of cognition classification consensus study. *Alzheimers Dement* 2018;14:280–92.
5 Ngolab J, Honma P, Rissman RA. Reflections on the utility of the retina as a biomarker for Alzheimer's disease: a literature review. *Neurol Ther* 2019;8:57–72.
6 Snyder PJ, Alber J, Alt C, *et al*. Retinal imaging in Alzheimer's and neurodegenerative diseases. *Alzheimers Dement* 2021;17:103–11.
7 Kashani AH, Chen C-L, Gahm JK, *et al*. Optical coherence tomography angiography: a comprehensive review of current methods and clinical applications. *Prog Retin Eye Res* 2017;60:66–100.
8 O'Bryhim BE, Apte RS, Kung N, *et al*. Association of preclinical Alzheimer disease with optical coherence tomographic angiography findings. *JAMA Ophthalmol* 2018;136:1242.
9 Bulut M, Kurtuluş F, Gözkaya O, *et al*. Evaluation of optical coherence tomography angiographic findings in Alzheimer's type dementia. *Br J Ophthalmol* 2018;102:233–7.
10 Yoon SP, Grewal DS, Thompson AC, *et al*. Retinal microvascular and neurodegenerative changes in Alzheimer's disease and mild cognitive impairment compared with control participants. *Ophthalmol Retina* 2019;3:489–99.
11 Lahme L, Esser EL, Mihailovic N, *et al*. Evaluation of ocular perfusion in Alzheimer's disease using optical coherence tomography angiography. *J Alzheimers Dis* 2018;66:1745–52.
12 Zabel P, Kaluzny JJ, Wilkosc-Debczynska M, *et al*. Comparison of retinal microvasculature in patients with Alzheimer's disease and primary open-angle glaucoma by optical coherence tomography angiography. *Invest Ophthalmol Vis Sci* 2019;60:3447–55.
13 Hong J, Yantao W, Yingying S, *et al*. Altered macular microvasculature in mild cognitive impairment and Alzheimer disease. *J Neuroophthalmol* 2017;1.
14 Wu J, Zhang X, Azhati G, *et al*. Retinal microvascular attenuation in mental cognitive impairment and Alzheimer's disease by optical coherence tomography angiography. *Acta Ophthalmol* 2020;98:e781–7.
15 Zhang YS, Zhou N, Knoll BM, *et al*. Parafoveal vessel loss and correlation between peripapillary vessel density and cognitive performance in amnestic mild cognitive impairment and early Alzheimer's disease on optical coherence tomography angiography. *PLoS One* 2019;14:e0214685.
16 Chua J, Hu Q, Ke M, *et al*. Retinal microvasculature dysfunction is associated with Alzheimer's disease and mild cognitive impairment. *Alzheimers Res Ther* 2020;12:161.
17 McKhann GM, Knopman DS, Chertkow H, *et al*. The diagnosis of dementia due to Alzheimer's disease: recommendations from the National Institute on Aging-Alzheimer's association workgroups on diagnostic guidelines for Alzheimer's disease. *Alzheimers Dement* 2011;7:263–9.
18 Albert MS, DeKosky ST, Dickson D, *et al*. The diagnosis of mild cognitive impairment due to Alzheimer's disease: recommendations from the National Institute on aging-Alzheimer's association workgroups on diagnostic guidelines for Alzheimer's disease. *Alzheimers Dement* 2011;7:270–9.
19 Ma Y, Hao H, Xie J, *et al*. Rose: a retinal OCT-angiography vessel segmentation dataset and new model. *IEEE Trans Med Imaging* 2021;40:928–39.
20 Hao J, Shen T, Zhu X, *et al*. Retinal structure detection in OCTA image via Voting-Based Multitask learning. *IEEE Trans Med Imaging* 2022;41:3969–80.
21 Xiao Y, Wu J, Lin Z, *et al*. A deep learning-based multi-model ensemble method for cancer prediction. *Comput Methods Programs Biomed* 2018;153:1–9.
22 Zhao Y, Zhang J, Pereira E, *et al*. Automated tortuosity analysis of nerve fibers in corneal confocal microscopy. *IEEE Trans Med Imaging* 2020;39:2725–37.
23 Xie J, Liu Y, Zheng Y. Classification of Retinal Vessels into Artery-Vein in OCT Angiography Guided by Fundus Images. In: *Medical image computing and computer assisted intervention – MICCAI*. Springer International Publishing, 2020: 117–27.
24 Domalpally A, Danis RP, White J, *et al*. Circularity index as a risk factor for progression of geographic atrophy. *Ophthalmology* 2013;120:2666–71.
25 Brown WR, Thore CR. Review: cerebral microvascular pathology in ageing and neurodegeneration. *Neuropathol Appl Neurobiol* 2011;37:56–74.
26 Fenner BJ, Tan GSW, Tan ACS, *et al*. Identification of imaging features that determine quality and repeatability of retinal capillary plexus density measurements in OCT angiography. *Br J Ophthalmol* 2018;102:509–14.
27 Spaide RF, Curcio CA. Evaluation of segmentation of the superficial and deep vascular layers of the retina by optical coherence tomography angiography instruments in normal eyes. *JAMA Ophthalmol* 2017;135:259–62.
28 Nesper PL, Fawzi AA. Human parafoveal capillary vascular anatomy and connectivity revealed by optical coherence tomography angiography. *Invest Ophthalmol Vis Sci* 2018;59:3858–67.
29 Campbell JP, Zhang M, Hwang TS, *et al*. Detailed vascular anatomy of the human retina by projection-resolved optical coherence tomography angiography. *Sci Rep* 2017;7:1–11.
30 Langa KM, Levine DA, Langa Kenneth M. The diagnosis and management of mild cognitive impairment: a clinical review. *JAMA* 2014;312:2551–61.
31 Linderman RE, Muthiah MN, Omoba SB, *et al*. Variability of foveal avascular zone metrics derived from optical coherence tomography angiography images. *Transl Vis Sci Technol* 2018;7:20.